DNA Repair 54 (2017) 30–39

Contents lists available at ScienceDirect

DNA Repair

journal homepage: www.elsevier.com/locate/dnarepair

hSSB1 phosphorylation is dynamically regulated by DNA-PK and PPP-family protein phosphatases

Nicholas W. Ashton[a,1], Nicolas Paquet[a], Sally L. Shirran[b], Emma Bolderson[a], Ruvini Kariawasam[c], Christine Touma[c], Azadeh Fallahbaghery[c], Roland Gamsjaeger[c], Liza Cubeddu[c], Catherine Botting[b], Pamela M. Pollock[a], Kenneth J. O'Byrne[a], Derek J. Richard[a,*]

[a] School of Biomedical Research, Institute of Health and Biomedical Innovation at the Translational Research Institute, Queensland University of Technology, 37 Kent Street, Woolloongabba 4102, QLD, Australia
[b] School of Biology, Biomedical Sciences Research Complex, University of St Andrews, North Haugh, St Andrews, Fife KY16 9ST, UK
[c] School of Science and Health, University of Western Sydney, Locked Bag 1797, Penrith 2751, NSW, Australia

ARTICLE INFO

Keywords:
hSSB1
DNA-PK
PPP-family phosphatase
Replication fork
Replication stress

ABSTRACT

The maintenance of genomic stability is essential for cellular viability and the prevention of diseases such as cancer. Human single-stranded DNA-binding protein 1 (hSSB1) is a protein with roles in the stabilisation and restart of stalled DNA replication forks, as well as in the repair of oxidative DNA lesions and double-strand DNA breaks. In the latter process, phosphorylation of threonine 117 by the ATM kinase is required for hSSB1 stability and efficient DNA repair. The regulation of hSSB1 in other DNA repair pathways has however remained unclear. Here we report that hSSB1 is also directly phosphorylated by DNA-PK at serine residue 134. While this modification is largely suppressed in undamaged cells by PPP-family protein phosphatases, S134 phosphorylation is enhanced following the disruption of replication forks and promotes cellular survival. Together, these data thereby represent a novel mechanism for hSSB1 regulation following the inhibition of replication.

1. Introduction

DNA replication constitutes one of the most important processes within the cell and allows for the accurate duplication of genomic information prior to cell division. While this process occurs rapidly in unperturbed cells, numerous endogenous and exogenous sources may either slow or stall replication fork progression [1]. Such disruption results in the exposure of single-stranded DNA (ssDNA) that must be stabilised to prevent replication fork collapse and double-stranded DNA break formation [2]. This process includes the nucleation of replication protein A (RPA) onto exposed ssDNA, as well as the subsequent accumulation and activation of the ataxia telangiectasia and Rad3-related (ATR) kinase [3]. ATR may then phosphorylate Chk1 to promote cell cycle checkpoint activation [4], as well as other proteins involved in restarting replication [5]. In addition to ATR, numerous additional regulatory enzymes are also activated by replication stress, including the related PI3K-like kinases, ataxia telangiectasia mutated (ATM) and DNA-dependent protein kinase (DNA-PK) [6–8]. Activation of these enzymes results in the coordinated regulation of numerous DNA repair proteins and is exemplified by the ATM, ATR and DNA-PK-mediated phosphorylation of the RPA 32 kDa subunit (RPA32) [8–10].

Recently our group and others provided evidence that the restart of stalled replication forks is promoted by human single-stranded DNA-binding protein 1 (hSSB1; also known as Nucleic Acid Binding Protein 2 NABP2) [11,12], a ssDNA-binding protein that also functions in the repair of double-stranded DNA breaks [13] and oxidative nucleotide lesions [14]. Following the disruption of replication, hSSB1 was found to localise with stalled replication forks where it promotes recruitment and subsequent activation of the ATR kinase. The importance of hSSB1 in these processes is highlighted by the inefficiency of hSSB1-depleted cells to activate checkpoint signalling following replication stress, as well as their inability to restart stalled replication forks. These deficiencies are manifested by hypersensitivity to multiple replication inhibitors [11].

Previous studies have indicated that hSSB1 may be phosphorylated at threonine residue 117 (T117) [13] and acetylated at lysine residue

* Corresponding author. Tel.: +61 734437236; Fax: +61 734437779.
E-mail addresses: nicholas.ashton@nih.gov (N.W. Ashton), nicholas.paquet@luinabio.com.au (N. Paquet), ss101@st-andrews.ac.uk (S.L. Shirran), emma.bolderson@qut.edu.au (E. Bolderson), R.Kariawasam@westernsydney.edu.au (R. Kariawasam), C.Touma@westernsydney.edu.au (C. Touma), A.Fallahbaghery@westernsydney.edu.au (A. Fallahbaghery), R.Gamsjaeger@westernsydney.edu.au (R. Gamsjaeger), L.Cubeddu@westernsydney.edu.au (L. Cubeddu), cb2@st-andrews.ac.uk (C. Botting), pamela.pollock@qut.edu.au (P.M. Pollock), k.obyrne@qut.edu.au (K.J. O'Byrne), derek.richard@qut.edu.au (D.J. Richard).
[1] The Eunice Kennedy Shriver National Institute of Child Health and Human Development, National Institutes of Health, 9800 Medical Center Drive, Rockville, MD 20850, USA

http://dx.doi.org/10.1016/j.dnarep.2017.03.006
Received 10 January 2017; Received in revised form 28 February 2017; Accepted 24 March 2017
Available online 06 April 2017

94 (K94) [15], both of which promote hSSB1 function in response to ionising radiation exposure. Mass spectrometry screens of proteins immunoprecipitated with phosphorylation and acetylation motif specific antibodies have also identified numerous other potentially modified hSSB1 residues, although these remain to be validated and have not been associated with any particular stress or cellular function [16]. Nevertheless, these findings support that hSSB1 may be highly regulated in cells through post-translational modifications.

In this study we describe the novel phosphorylation of hSSB1 residue S134 by the central DNA repair kinase DNA-PK and suggest that this modification is important for hSSB1 function following replication fork inhibition.

2. Materials and methods

2.1. Plasmids and site-directed mutagenesis

The 3x FLAG hSSB1 mammalian expression vector (3DDK-AN-pCMV6) has been described previously [14], as has the pET28A hexa-His-hSSB1 *E. coli* expression construct [13]. Site directed mutagenesis was used to prepare S134A and siRNA resistant hSSB1 as previously described [17] using the following primer sets: S134A (F) 5′- GCAACCCTTCAGCT**G**CCCAGCCTACCAC-3′, (R) 5′-GTGGTAGGCTGGG**C**AGCTGAAGGGTTGC-3′; S134E (F) 5′-CAGCAACCCTTCAGCT**GAG**CAGCCTACCACTGGAC-3′, (R) 5′-GTCCAGTGGTAGGCTG**CTC**AGCTGAAGGGTTGCTG-3′; siRNA resistance (F) 5′-CAGGCCCGCCTGGCCCTTCTTCCAATCCCGTTAGTAACGGCAAAGAAAC-3′, (R) 5′-GTTTCTTTGCCGTTACTAACGGGATTGGAAGAAGGGCCAGGCGGGCCTG-3′.

2.2. Cell culture and treatments

HeLa and HEK293T cell cultures were maintained in Roswell Park Memorial Institute medium (RPMI, Sigma-Aldrich) supplemented with 10% foetal bovine serum (Sigma-Aldrich) and cultured in a humidified incubator with 5% CO_2 at 37 °C. Stealth siRNA of the following sequence 5′-GCCCUUCCAGCAACCCUGUUAGUAA-3′ was used to deplete hSSB1 from cells. Silencer Select siRNA (Life Technologies) of sequence 5′- CAAGCGACUUUAUAGCCUUTT-3′ was used to depleted DNA-PKcs. Stealth siRNA negative control med GC, or Silencer Select negative control no.1, were used as negative control siRNAs where appropriate. Stealth siRNA was used at a concentration of 50 nM, and Silence Select siRNA at 10 nM. Mammalian expression vectors were transfected using Lipofectamine 2000 (Life Technologies) or FuGENE HD (Promega) and siRNA were transfected using Lipofectamine RNAiMax (Life Technologies). Hydroxyurea, aphidicolin, thymidine and camptothecin were purchased from Sigma-Aldrich. KU-60019, VE-821 and NU7441, inhibitors of ATM, ATR and DNA-PK, respectively, were purchased from Selleck Chemicals. KU-60019 and NU7441 were used at a final concentration of 5 μM and VE-821 at 10 μM. Okadaic acid and calyculin A were purchased from Cell Signaling Technology. Okadaic acid was added to cells at concentrations of 25 nM or 1 μM. Calyculin A was added to cells at a final concentration of 50 nM. Double-strand DNA breaks were induced in cells by exposure to 6 Gy ionising radiation using a Gammacell 40 Exactor caesium-source irradiator.

2.3. Clonogenic survival assays

Clonogenic survival assays were performed as described previously [14]. Briefly, HeLa cells were depleted of hSSB1 by transfection with siRNA twice, separated by a 24 h interval, prior to transient expression of siRNA-resistant WT, S134A or S134E 3x FLAG hSSB1 24 h later. Cells were then seeded into wells of a 6-well plate (each dose in triplicate) at a density of 400 cells per well. 24 h subsequent to over-expression, cells were treated with 3 mM hydroxyurea or 6 μg μl^{-1} aphidicolin (B) for 4, 8, 12, 16 or 20 h, or left untreated, prior to washing 2x with PBS and exchanging with fresh media. Alternatively, cells were treated with increasing concentrations of camptothecin (50, 100, 150 or 200 nM) for 1 h prior to media exchange, or with increasing doses of ionising radiation (1, 2, 4 or 6 Gy). Cells were grown for 10 days post-treatment prior to staining of colonies with methylene blue. Colonies were manually counted and normalised to untreated cells. Each assay was performed four times and results presented as the mean ± 1 standard deviation (SD). Unpaired, two-tailed *t* tests were performed using the Holm–Sidak method to assess statistical significance between individual data sets at each dose using GraphPad Prism version 6 software. $p < 0.05$ was considered statistically significant.

2.4. Cell lysis, immunoblotting and antibodies

Whole cell lysates were prepared by lysis in Radioimmunoprecipitation buffer (RIPA buffer; 50 mM Tris pH 8.0, 150 mM NaCl, 0.1% SDS, 0.5% sodium deoxycholate, 1% Triton X100) supplemented with 1x phosphatase inhibitor cocktail (Cell Signaling Technology) and 1x protease inhibitor cocktail (cOmplete, EDTA free; Roche), followed by sonication (Vibra-Cell, 3 mm probe; Sonics and Materials), with 3x 3 s bursts (10% output). 15-20 μg of whole cell lysate was typically separated by electrophoresis on a 4–12% Bis-Tris Plus Bolt precast gel (Life Technologies) and transferred to nitrocellulose.

Commercial antibodies against the following targets were purchased from Cell Signaling: p-S345 Chk1 (1:500, clone 133D3, cat # 2348), Chk1 (1:500, clone 2G1D5, cat # 2360), p-T68 Chk2 (1:500, clone C13C1, cat # 2197), Chk2 (1:500, clone 1C12, cat # 3440), DNA-PKcs (1:500, clone 3H6, cat # 12311), p-S1981 ATM (1:500, clone D6H9, cat # 5883), ATM (1:500; clone D2E2, cat # 2873), ATR (1:500, clone E1S3S, cat # 13934) and RPA32 (1:1000, clone 4E4, cat # 2208). The antibodies against p-S33 RPA32 (1:1000, cat # A300-46A) and p-S4/S8 RPA32 (1:2000, cat # A300-245A) were purchased from Bethyl, the FLAG antibody (1:2000; clone M2, cat # F1804) from Sigma-Aldrich, the p-S1989 ATR antibody (1:500; cat # GTX128145) from GeneTex and the Actin antibody (1:10,000 clone C4, cat # 612656) from BD Biosciences. The hSSB1 antibody was affinity purified from previously described sheep anti-serum [13] using recombinant WT hexa-His-hSSB1 bound to cyanogen-bromide activated sepharose beads (Sigma-Aldrich) as per the manufacturer's instructions.

To detect pS134 hSSB1, a polyclonal antibody was raised against the hSSB1 peptide PSA{pS}QPTTGPKC (GenScript). To prevent non-specific binding of the antibody to non-phosphorylated hSSB1, a 200x molar excess of a control peptide (PSAQPTTGPKC) was included in all antibody working-solutions. A 200x molar excess of phosphorylated peptide was used to block the antibody from binding pS134 hSSB1 in Fig. 3B. For validation of the antibody, whole cell lysates were dephosphorylated by addition of 200 Units of lambda (λ) phosphatase (New England Biolabs) and incubation at 30 °C for 45 min.

Primary antibodies were detected using IRDye 680RD or 800CW-conjugated donkey anti-mouse, rabbit, goat or rat fluorescent secondary antibodies (Li-Cor) and visualised using the Odyssey Imaging system (Li-Cor). When necessary, immunoblots were quantified using ImageJ software. Phosphorylation of hSSB1 S134 was expressed relative to total immunoprecipitated endogenous hSSB1, or to total 3x FLAG hSSB1, as appropriate. RPA32 phosphorylation was calculated as the relative ratio of the 34–32 kDa RPA32 bands.

2.5. Immunoprecipitation

Cells were lysed by sonication in immunoprecipitation buffer (20 mM HEPES pH 7.5, 150 mM KCl, 5% glycerol, 10 mM $MgCl_2$, 0.5% Triton X-100) supplemented with 1x phosphatase inhibitor cocktail, 1x protease inhibitor cocktail and Benzonase (1:1000, Sigma-Aldrich). For immunoprecipitation of hSSB1, protein G magnetic dynabeads (Life Technologies) were prepared by incubation with the

hSSB1 antibody or with an isotype control IgG (Sigma). Alternatively, for the precipitation of FLAG-tagged proteins, magnetic anti-FLAG M2 beads (Sigma-Aldrich) were resuspended and prepared by washing in immunoprecipitation buffer. In either instance, whole cell lysates were incubated with antibody-bound beads for 2 h at 4 °C, beads washed 5x with immunoprecipitation buffer and proteins eluted by heating to 80 °C for 5 min in 3x SDS loading dye. Eluted proteins were separated by electrophoresis and either immunoblotted or stained with colloidal Coomassie blue.

2.6. Mass spectrometry

Gel bands were excised and cut into 1 mm cubes. These were then subjected to in-gel digestion using a ProGest Investigator in-gel digestion robot (Digilab) using standard protocols [18]. Briefly, the gel cubes were destined by washing with acetonitrile and subjected to reduction and alkylation before digestion with trypsin at 37 °C. The peptides were extracted with 5% formic acid and concentrated to a volume of 20 μL, using a SpeedVac (ThermoSavant). Peptides were then separated on an Acclaim PepMap 100 C18 trap and an Acclaim PepMap RSLC C18 column (ThermoFisher Scientific), using a nanoLC Ultra 2D plus loading pump and nanoLC as-2 autosampler (Eksigent). A quarter (5 μL) of the sample was loaded. Peptides were eluted with a gradient of increasing acetonitrile, containing 0.1% formic acid (5–40% acetonitrile in 5 min, 40–95% in a further 1 min, followed by 95% acetonitrile to clean the column, before re-equilibration to 5% acetonitrile). The eluate was sprayed into a TripleTOF 5600 electrospray tandem mass spectrometer (ABSciex) and analysed in Information Dependent Acquisition (IDA) mode, performing 250 msec of MS followed by 150 msec MSMS analyses on the 15 most intense peaks seen by MS. The MS/MS data file generated was analysed using the Mascot algorithm (Matrix Science) against the NCBI non-redundant (nr) database July 2014 with no species restriction, trypsin as the cleavage enzyme, carbamidomethyl as a fixed modification of cysteines and methionine oxidation, deamidation of glutamines and asparagines and phosphorylation of serine, threonine and tyrosine as a variable modifications.

The raw mass spectrometry data and Mascot search files have been deposited to the ProteomeXchange Consortium via the PRIDE partner repository [19] with the dataset identifier PXD003964.

2.7. Protein purification

SHuffle® T7 Competent *E. coli* were transformed with plasmids encoding WT, S134A or S134E hexa-His-hSSB1. Proteins were prepared as previously described [14]. Concentrations of fully reduced monomeric hSSB1 were estimated on SDS-PAGE gels.

2.8. DNA-PK kinase assay

10 U of purified DNA-PK (Promega) was incubated with 500 ng of recombinant hSSB1 in 50 μL of kinase buffer (20 mM HEPES, 50 mM NaCl, 10 mM $MgCl_2$, 10 mM MnCl, 1 mM DTT) containing 100 μM ATP and 10 μg mL^{-1} sonicated salmon sperm DNA (Invitrogen). Reactions were incubated for 30 minutes at 30 °C and then stopped by addition of 3x SDS loading dye containing 20% β-mercaptoethanol and heating to 80 °C for 5 min. Samples were electrophoresed in duplicate and either stained with colloidal coomasie brilliant blue or immunoblotted.

2.9. One dimensional nuclear magnetic resonance spectroscopy (1D-NMR)

WT, S134A or S134E hexa-His hSSB1 (~ 100-200 μM) was resuspended in NMR buffer (20 mM Tris pH 6.9, 100 mM NaCl, 1 mM EDTA, 1 mM TCEP) with 10% ^2H_2O and analysed at 298 K on a Bruker 600 Mhz spectrometer (Bruker Avance III; Bruker) equipped with a 5 mm TCI cryoprobe. Proton chemical shifts are references to 4,4-dimethyl-4-silapentanesulfonic acid (DSS) at 0 ppm. Data were processed using Topspin software (Bruker).

2.10. Synthetic DNA substrates

Biotin-labelled oligonucleotides were purchased from Integrated DNA Technologies (IDT). The ssDNA and fork junction substrates have been described previously [20]. Substrates were annealed and purified as previously described [21]. Briefly, individual oligonucleotides were firstly isolated on 12% polyacrylamide, 8 M urea gels and eluted by overnight passive diffusion in TE buffer. Equimolar quantities of oligonucleotides were then mixed in hybridisation buffer (50 mM Tris pH 7.5, 100 mM NaCl, 10 mM $MgCl_2$), heated at 99 °C for 10 min and slowly cooled to room temperature. Annealed structures were purified on 10% polyacrylamide gels, electro-eluted and concentrated using EMD Millipore *Amicon Ultra*-4 centrifugal filter units with a 3 kDa cut-off. Substrate concentrations were determined from absorbance at 260 nm. Here, the oligonucleotide molar extinction coefficients were calculated by a nearest neighbour approach, taking into account the hypochromicity of dsDNA.

2.11. BioLayer interferometry (BLI)

DNA-binding studies with WT and S134E recombinant hSSB1 were performed using a set of seven protein concentrations (6, 4, 2, 1, 0.5, 0.25 and 0.125 μM). Proteins were bound to immobilised 5′-biotinylated DNA constructs (ssDNA and fork-DNA) in triplicate, using the BLItz system (ForteBio). Streptavidin biosensors (ForteBio) were equilibrated in DNA buffer (10 mM Tris-HCl, 1 mM EDTA, pH 8) prior to use. For each individual binding curve, an initial 20 s baseline was performed followed by loading of the biotinylated DNA construct until saturation (120 s). Two further baselines (20 s each) were carried out to transition from the DNA buffer to protein buffer (10 mM phosphate, 50 mM NaCl, 3 mM TCEP, pH 7.5). Both WT and S143E hSSB1 were allowed 120 s for association, followed by a 20 s dissociation step. The interaction response level for each binding was calculated by the difference between the maximum and minimum BLI values for each binding curve. These values were plotted against the corresponding protein concentration and fitted to a steady-state binding model using the hill equation ($n = 1$).

3. Results

3.1. Mass spectrometric detection of phosphorylated hSSB1

To further understand the post-translational regulation of hSSB1, 3x FLAG hSSB1 was immunoprecipitated from HEK293T cells treated with or without 3 mM hydroxyurea (HU) for 4 h and separated by SDS-PAGE (Fig. 1A). Bands corresponding to 3x FLAG hSSB1 of ~ 30 and 35 kDa were then excised from the gel and subjected to in-gel trypsin digestion. The resulting peptides were distinguished by qualitative electrospray ionisation tandem mass spectrometry (ESI-MS/MS) and results analysed using the Mascot algorithm against the NCBI database. N- and C-terminal hSSB1 peptides were identified for the ~ 30 and 35 kDa bands, suggesting that both species represent full-length hSSB1 (Fig. S1A). Potentially phosphorylated serine and threonine residues were identified from both bands analysed for each sample (Figs. 1B and S1B). This included detection of a phosphorylated peptide corresponding to residues 124–178. Whilst the MS/MS fragmentation of this peptide was not conclusive enough to confidently determine the site of phosphorylation (Fig. S1C and S1D), we noted that S134 is a component of an SQ motif. SQ and TQ motifs are often present in DNA repair proteins where they may be substrates of the DNA repair P13K-like kinases, ATM, ATR and DNA-PK. Indeed, phosphorylation of hSSB1 T117, a TQ motif, has previously been described [13]. We therefore reasoned that S134 phosphorylation might also regulate hSSB1 during DNA repair.

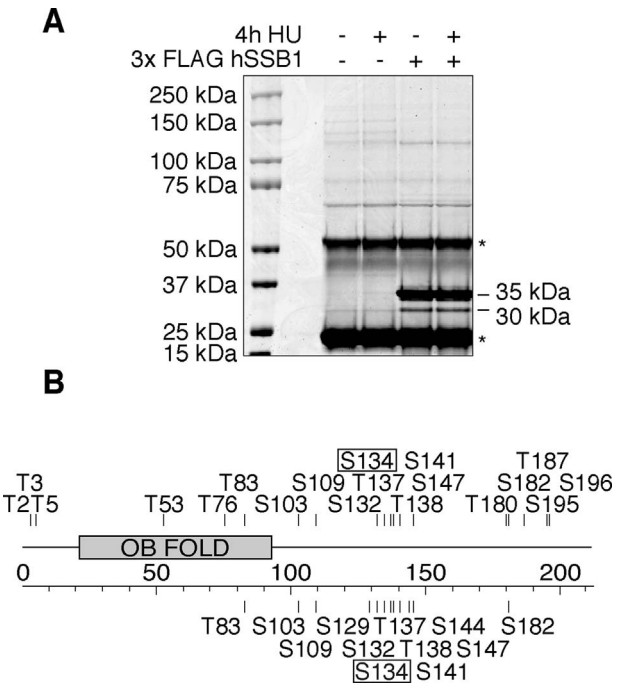

Fig. 1. Detection of phosphorylated hSSB1 by mass spectrometry **(A)** HEK293T cells were transiently transfected with 3x FLAG hSSB1 or an empty plasmid 24 h prior to treatment with 3 mM hydroxyurea (HU) for 4 h. 3x FLAG hSSB1 was immunoprecipitated from 12 mg of whole cell lysate using M2 FLAG magnetic beads and separated on a BOLT precast gel. The gel was stained using colloidal Coomassie blue G-250 and is shown in greyscale. * = M2 FLAG IgG proteins **(B)**. Gel slices containing 3x FLAG hSSB1 were excised and digested with trypsin. Peptides were detected by ESI-MS/MS and data analysed using the Mascot algorithm against the NCBI non-redundant (nr) database. Putative phosphorylation sites detected prior to HU treatment are indicated above the hSSB1 schematic, while those detected after treatment is indicated below. OB fold = oligonucleotide/oligosaccharide-binding fold.

3.2. Cells expressing S134A hSSB1 are more sensitive to replication fork disruption and double-strand DNA break formation

To determine whether S134 phosphorylation may be important for the function of hSSB1, clonogenic assays were performed using cells depleted of endogenous hSSB1 and transiently expressing siRNA-resistant WT or phospho-mutant S134A 3x FLAG hSSB1 (Fig. 2A). Initially, cells were incubated with 3 mM hydroxyurea for 4, 8, 12, 16 or 20 h. Consistent with our previously published data [11], hSSB1-depleted cells were hypersensitive to hydroxyurea treatment, which could be rescued by re-introduction of exogenous WT hSSB1. Over expression of S134A hSSB1 was however unable to rescue the sensitivity associated with hSSB1 depletion (Fig. 2B). HU suppresses new DNA replication through the inhibition of ribonucleotide reductase and the disruption of dNTP synthesis within the cell [22]. To confirm that our findings were due to fork disruption and not indirect effects of HU treatment, cells were also treated with 6 μg μL^{-1} of the DNA polymerase α inhibitor aphidicolin (Aph) for the same time periods. Similarly to HU treatment, hSSB1-depleted cells were hypersensitive to treatment with Aph, which could be rescued by re-introduction of WT, although not of S134A, siRNA-resistant 3x FLAG hSSB1 (Fig. 2C).

In addition to the cellular response to replication fork stalling, hSSB1 has also been implicated in the repair of collapsed replication forks [11], as well as in the repair of double-strand DNA breaks throughout the cell cycle [13]. To evaluate whether hSSB1 S134 phosphorylation may also promote cellular survival in response to these damage events, cells were also treated with increasing doses of the topoisomerase I inhibitor, camptothecin (Fig. 2D; to cause replication-associated double-strand DNA-breaks), or exposed to increasing doses of ionising radiation (Fig. 2E; to induce double-strand DNA-breaks non-specifically). As expected, hypersensitivity to either stress was observed in those cells depleted of hSSB1, which could be rescued by transient expression of siRNA-resistant WT 3x FLAG hSSB1. Cells expressing siRNA-resistant S134A 3x FLAG hSSB1 were however similarly sensitive to those depleted of hSSB1. These data thereby suggest that as well as in response to replication fork stalling, hSSB1 S134 phosphorylation may also be required for cellular survival following double-strand DNA-break formation. One-dimensional NMR analysis of recombinant WT and S134A hexa-His-hSSB1 suggested that this sensitivity was not due to misfolding of the S134A mutant and was indeed likely due to a functional requirement of S134 phosphorylation following DNA damage (Fig. S2A).

It is interesting to note that while S134 and T117 are highly conserved in primates, they are less so in other animals (Fig S3A). Indeed, serine is not present at residue 134 in either mice or rats. These observations may be consistent with the previously reported functional discrepancies between human and murine SSB1 orthologues [23], which presumably undergo differential regulation. Despite the lack of site-specific conservation of an SQ motif at S134, we did however notice amongst the vast majority of species examined, the presence of one or more SQ/TQ motifs within an ~ 40 amino acid region from residue 117 to 160. This observation may suggest that in those species not phosphorylated at S134 or T117, regulation may instead be achieved by phosphorylation of an alternative proximal residue. In addition, we noted that unlike hSSB1, hSSB2 does not contain SQ or TQ motifs (Fig S3B). This is consistent with suggestions that hSSB1 regulation may be more complex than that of hSSB2, as is also evidenced by the reported lack of detectable hSSB2 acetylation [15].

3.3. Immunodetection of S134 phosphorylation in response to replication stress

As our data now suggest that hSSB1 is likely phosphorylated at S134, we sought to confirm this by immunodetection. A rabbit polyclonal antibody was therefore generated using a S134 phosphorylated peptide representing hSSB1 residues 131–140. Using this antibody, phosphorylation of immunoprecipitated endogenous hSSB1 could be detected following HU treatment, in a time-dependent manner (Fig. 3A). Phosphorylation was however most readily detected by immunoblotting of whole cell lysates from HeLa cells transiently expressing WT 3x FLAG hSSB1 (Fig. 3B). An increase in S134 phosphorylation was also detected for transiently expressed hSSB1, increasing for up to 20 h post-HU addition. Here, hSSB1 was phosphorylated at a similar rate to RPA32 (Fig. 3C), another ssDNA-binding protein that is rapidly phosphorylated following replication stress [24]. Specificity of the pS134 antibody for phosphorylated hSSB1 was confirmed by expression of a S134A 3x FLAG hSSB1 mutant, as well as by treatment of whole cell lysates with lambda phosphatase (λPPase) and by use of a phosphorylated peptide to block antigen recognition by the antibody (Fig. 3B). Specificity was further enhanced by inclusion of a non-phosphorylated control peptide of otherwise identical sequence to the blocking peptide in all phospho-antibody working solutions. An increase in hSSB1 S134 phosphorylation was also observed following treatment of cells with 6 μg μL^{-1} aphidicolin for 4, 8 and 12 h (Fig. 3D), or with 1 μM camptothecin for 1 h (Fig. 3E).

In addition to the response to replication inhibition, hSSB1 also functions in the repair of double-stranded

DNA breaks. We therefore reasoned that hSSB1 might also be phosphorylated following the formation of these lesions. To assess this, HeLa cells expressing WT 3x FLAG hSSB1 were exposed to 6 Gy of ionising radiation and collected after 0.5, 1, 2 or 4 h. Whilst robust phosphorylation of ATM S1981 was induced by this treatment, indicating the induction of DNA damage [25], it failed to elicit an hSSB1 S134 phosphorylation response which was comparable to 4 h treatment with 3 mM hydoxyurea (Fig. 3F).

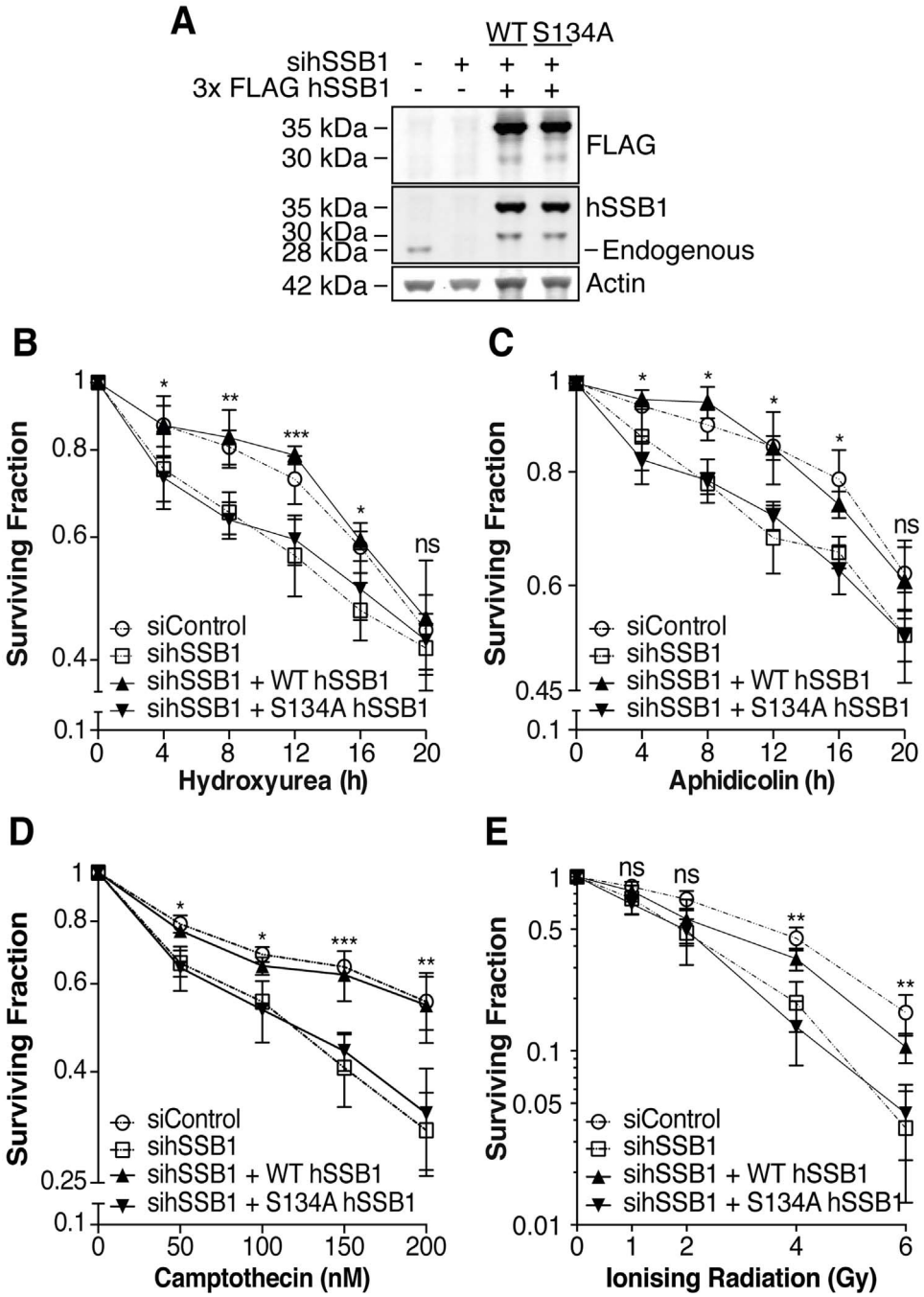

Fig. 2. Cells expressing S134A hSSB1 are more sensitive to replication fork disruption. **(A)** HeLa cells were depleted of hSSB1 using siRNA (sihSSB1) and then transfected with WT or S134A siRNA-resistant 3x FLAG hSSB1. After 6 h, cells were seeded into wells of a 6-well plate. Remaining cells were grown for an additional 24 h and analysed by immunoblotting. **(B, C, D and E)** The cells plated in **(A)** were incubated for 24 h and treated with 3 mM hydroxyurea (B) or 6 μg μL^{-1} aphidicolin **(C)** for 4, 8, 12, 16 or 20 h, or with 50, 100, 150, 200 or 250 nM camptothecin for 1 h **(D)**, prior to exchanging with fresh media. Alternatively, cells were exposed to, 1, 2, 4, or 6 Gy ionising radiation **(E)**, or left untreated. Cells were grown for 10 days prior to staining of colonies with methylene blue. Colonies were manually counted and normalised to untreated cells. Data is graphed as the mean ± 1 standard deviation from four independent experiments. *t* tests were used to compare the 'sihSSB1 + WT hSSB1′ and "sihSSB1 + S134A hSSB1′ datasets at each dose. ns = $p > 0.05$, * = $p < 0.05$, ** = $p < 0.01$, *** = $p < 0.001$.

3.4. hSSB1 S134 phosphorylation is predominantly mediated by DNA-PK

To determine whether hSSB1 S134 may be a substrate of ATM, ATR or DNA-PK, HeLa cells transiently expressing 3x FLAG hSSB1 were pre-treated with chemical inhibitors against each of these kinases 30 min prior to addition of 3 mM HU for 4 h. While we consistently observed a small decrease in hSSB1 phosphorylation following addition of KU-60019 and VE-821 (inhibitors of ATM and ATR, respectively), a ~ 90% reduction in both basal and HU-induced hSSB1 phosphorylation was observed following treatment of cells with the DNA-PK inhibitor NU7441 (Fig. 4A and 4B). The efficacy of KU-60019 and VE-821 treatment to suppress ATM and ATR kinase activity was here confirmed by the prevention of ATM and ATR auto-phosphorylation, as well as the phosphorylation of Chk2 T68 (for ATMi; Fig S4A) and Chk1 S345 (for ATRi; Fig S4B), in response to genotoxic stress. As few unique DNA-PK substrates have been described, the efficacy of NU7441 to inhibit DNA-PK was instead confirmed by the ability, when co-treated with ATMi, to limit phosphorylation of RPA32 S4/S8 following HU exposure (Fig

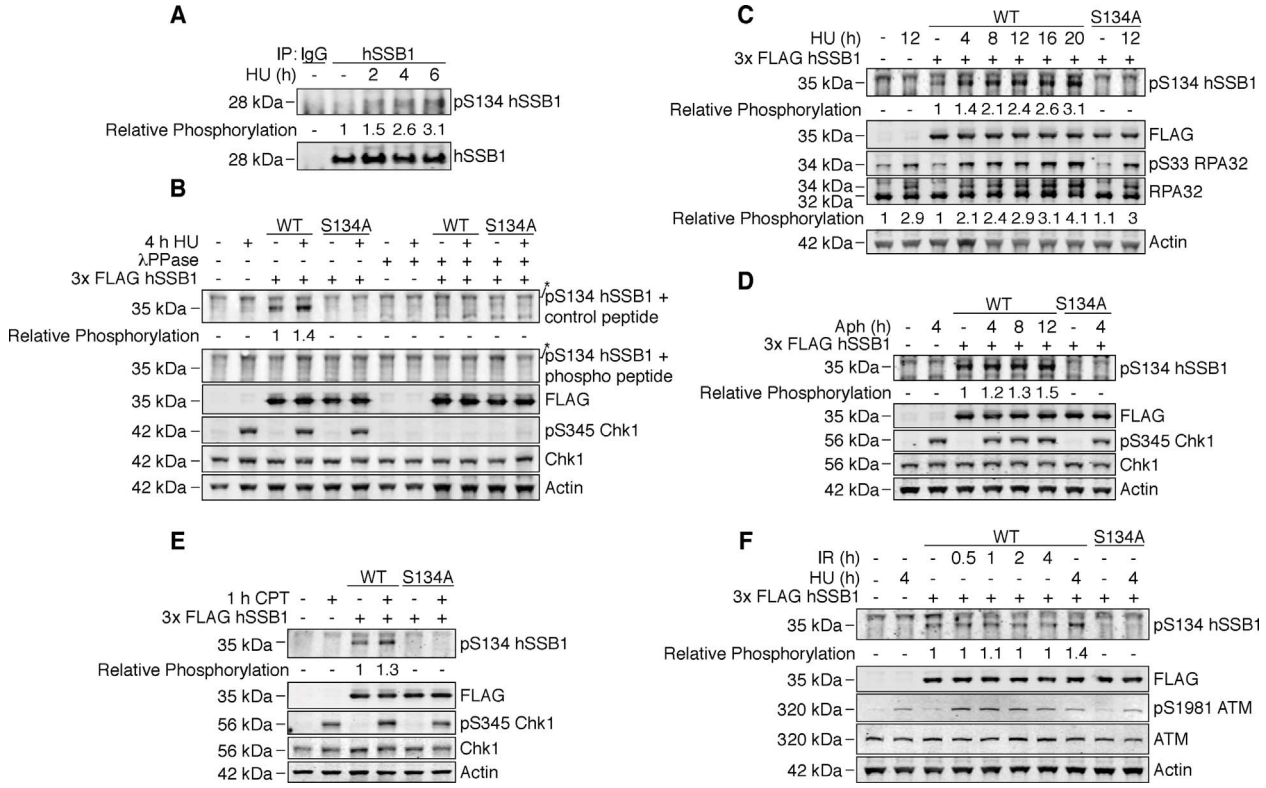

Fig. 3. hSSB1 is phosphorylated at S134 following replicative stress. **(A)** hSSB1 was immunoprecipitated from HeLa cells that had been treated with 3 mM HU for 2, 4 or 6 h, or mock-treated. Eluted proteins were immunoblotted for total and S134 phosphorylated hSSB1. Phosphorylation of hSSB1 S134 is expressed relative to total immunoprecipitated endogenous hSSB1. **(B)** HeLa cells were transfected with WT or S134A 3x FLAG hSSB1, or a vector control, 24 h prior to treatment of cells with 3 mM HU for 4 h. Whole cell lysates were prepared from these cells and incubated either with or without addition of lambda (λ) phosphatase at 30 °C for 45 min. Whole cell lysates were then immunoblotted and probed with a polyclonal antibody raised against the hSSB1 peptide PSA{pS}QPTTGPKC, representing hSSB1 phosphorylated at S134. To confirm specificity for S134 phosphorylated hSSB1, the antibody was pre-incubated for 30 min either with a control non-phosphorylated peptide (+ control peptide) or with the phosphorylated immunisation peptide (+ phospho peptide). Phosphorylation of Chk1 S345 was used as a positive control for HU treatment, as well as for lambda phosphatase activity. Actin served as a loading control. Phosphorylation of hSSB1 S134 is expressed relative to 3x FLAG hSSB1. * = non-specific band. **(C)** HeLa cells transiently expressing WT or S134A 3x FLAG hSSB1, or an empty vector, for 24 h were treated with 3 mM HU for 4, 8, 12, 16 or 20 h, or left untreated and then harvested. Whole cell lysates were prepared and analysed by immunoblotting. Phosphorylation of hSSB1 S134 is expressed relative to 3x FLAG hSSB1. Phosphorylation of RPA32 is expressed as the relative ratio of the 34 kDa to 32 kDa RPA32 bands. **(D and E)** HeLa cells were transfected with WT or S134A 3x FLAG hSSB1, or a vector control, 24 h prior to treatment of cells with 6 μg μL^{-1} aphidicolin (Aph) for 4, 8, or 12 h (D) or with 1 μM camptothecin (CPT) for 1 h **(E)**. Whole cell lysates prepared from these cells were analysed by immunoblotting. Phosphorylation of hSSB1 S134 is expressed relative to 3x FLAG hSSB1. **(F)** HeLa cells transiently expressing WT or S134A 3x FLAG hSSB1, or an empty vector, for 24 h were treated with 3 mM HU for 4 h, or exposed to 6 Gy of ionising radiation and harvested after 0.5, 1, 2 or 4 h. Whole cell lysates were prepared and analysed by immunoblotting. Phosphorylation of hSSB1 S134 is expressed relative to 3x FLAG hSSB1. Phosphorylation of ATM S1981 is used as a positive control for ionising radiation exposure.

S4C). The reduction in hSSB1 S134 phosphorylation observed with DNA-PKi was also supported by similar suppression in cells depleted of the DNA-PK catalytic subunit (DNA-PKcs) using siRNA (Fig. 4C). These data support that while ATM and ATR may have minor roles in the regulation of hSSB1 S134 phosphorylation, DNA-PK is most likely the major required kinase in cells, functioning both prior to and following replication fork disruption.

To investigate further whether DNA-PK may directly phosphorylate hSSB1 S134, we next performed an *in vitro* kinase assay using purified DNA-PK and recombinant hexa-His-hSSB1. Here we observed robust phosphorylation of WT hexa-His-hSSB1, although not of a S134A hexa-His-hSSB1 mutant, which was substantially increased following stimulation of DNA-PK activity by the addition of sonicated DNA (Fig. 4D). The relevance of this assay in cells was further supported by co-immunoprecipitation of DNA-PKcs with endogenous hSSB1, indicating that DNA-PK may be spatially available to act on hSSB1 in cells (Fig. 4E). In these assays, whole cell lysates were treated with the nuclease benzonase, to exclude any associations mediated by DNA. Here, association was observed both before and following HU treatment, suggesting that hSSB1 and DNA-PK may form a complex independently of exogenous DNA damage. Indeed, these observations are consistent with our finding that DNA-PKcs depletion or inhibition reduces both HU-induced and basal hSSB1 S134 phosphorylation. These findings provide evidence that hSSB1 is regulated by direct DNA-PK phosphorylation of S134, which is enhanced following replication fork disruption.

3.5. hSSB1 S134 phosphorylation is enzymatically suppressed

In undamaged cells, several DNA repair proteins, including Chk1 and ATM are maintained in a hypo-phosphorylated state through the function of PPP-family serine/threonine phosphatases (protein phosphatases (PP) 1, 2A, 4, 5, 6) [26,27]. As our data suggest that hSSB1 S134 may be partially phosphorylated in undamaged cells and then enhanced following replication stress, we reasoned that steady-state hSSB1 phosphorylation might also be subject to enzymatic suppression. To test this, HeLa cells transiently expressing 3x FLAG hSSB1 were treated with 3 mM hydroxyurea for 3.5 h, or mock treated, and then incubated with the PPP-family phosphatase inhibitors okadaic acid (OA) or calyculin A (CA) for 30 min (Fig. 5A). Strikingly, the treatment of undamaged cells with 1 μM OA, which inhibits > 95% of PP2A activity (as well the activity of PP4 and PP6) [26], or 50 nM CA, which additionally inhibits PP1 and PP5 (as observed by Chk1 phosphorylation) [28], lead to an increase in hSSB1 S134 phosphorylation of greater than 5- and 9-fold, respectively (Fig. 5A and B). Similar CA-induction of S134 phosphorylation was also detected for immunoprecipitated endogenous hSSB1 (Fig. 5C). An increase in hSSB1 S134 phosphorylation of ~ 5 fold was further observed within 5 min of CA treatment,

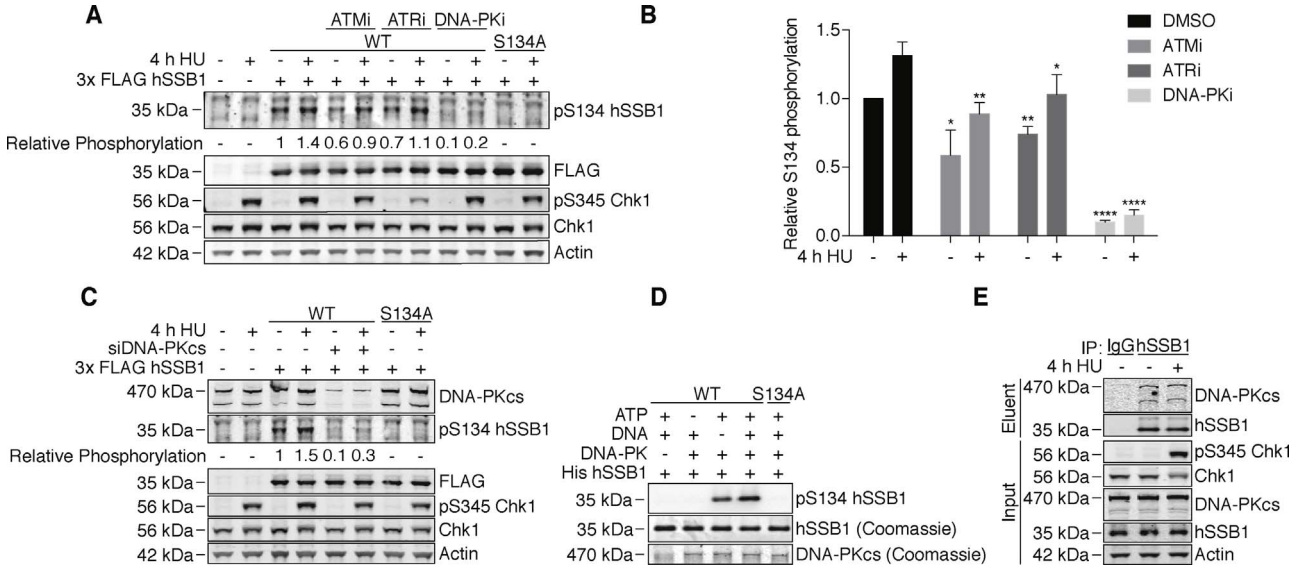

Fig. 4. hSSB1 S134 is phosphorylated by DNA-PK. **(A)** HeLa cells transiently expressing WT or S134A 3x FLAG hSSB1, or an empty vector, for 24 h were pre-treated with 5 μM KU-60019 (ATMi), 10 μM VE-821 (ATRi), 5 μM NU7441 (DNA-PKi), or DMSO (control) for 30 min, prior to treatment with 3 mM HU for 4 h. Whole cell lysates were then prepared and analysed by immunoblotting. Phosphorylation of hSSB1 S134 is expressed relative to 3x FLAG hSSB1. **(B)** Bar graph illustrating relative hSSB1 S134 phosphorylation from 3 independent repeats of **(A)**. Data is graphed as the mean ± 1 standard deviation. *t* tests were used to compare phosphorylation of hSSB1 S134 for each inhibitor data set relative to DMSO lanes for each dose. * = $p < 0.05$, ** = $p < 0.01$, *** = $p < 0.001$, **** = $p < 0.0001$. **(C)** DNA-PKcs was depleted from HeLa cells by transfection with 10 nM Silencer Select siRNA twice, separated by 24 h incubation, followed by transient expression of WT or S134A 3x FLAG hSSB1, or an empty control, after an additional 24 h. Cells were then treated with 3 mM HU for 4 h and whole cell lysates analysed by immunoblotting. Phosphorylation of hSSB1 S134 is expressed relative to 3x FLAG hSSB1. **(D)** 500 ng of recombinant WT or S134A hexa-His-hSSB1 was incubated with 10 U of DNA-PKcs/Ku for 30 min at 30 °C ± 100 μM ATP and 10 μg mL^{-1} sonicated salmon sperm DNA. Reactions were separated by PAGE and either immunoblotted for hSSB1 S134 phosphorylation or stained with colloidal Coomassie blue (shown in greyscale). **(E)** hSSB1 was immunoprecipitated from whole cell lysates of HeLa cells treated ± 3 mM HU for 4 h. Eluent nd whole cell lysate (2% input) was immoblotted as indicated.

indicating the rapidity of this reaction (Fig. 5D). These findings are particularly notable when it is considered that even after 20 h of HU treatment, an increase of only 3.1 fold was observed (Fig. 3C).

In addition to the clear overall increase in S134 phosphorylation observed following PPP-family phosphatase inhibition, the increase in S134 phosphorylation observed following HU-treatment was also found to be significantly greater in cells treated with 1 μM OA or 50 nM CA (Fig. 5A and B). These data may suggest that of the hSSB1 that is phosphorylated after HU treatment, a large amount may be subsequently dephosphorylated, even during conditions of fork disruption. As these observations indicate that hSSB1 S134 is also dynamically phosphorylated and dephosphorylated during the response to replication inhibition, we further reasoned that a similar dynamic phosphorylation response might explain the lack of detectable S134 phosphorylation observed in response to IR exposure (Fig. 3F), despite the apparent involvement of S134 phosphorylation in cellular survival following such stress (Fig. 2E). To test this, we again exposed cells expressing WT or S134A 3x FLAG hSSB1 to ionising radiation and then co-treated with 50 nM CA 30 min prior to harvesting (Fig. 5E and F). Whilst we again did not observe an IR-induced increase in S134 phosphorylation in non-CA treated cells, a marked increase in S134 phosphorylation was readily detected in those cells in which phosphatases had been inhibited. These data thereby suggest that hSSB1 S134 may be increasingly phosphorylated in response to DNA damage, including in response to IR treatment, although that opposing dephosphorylation may also concurrently occur.

3.6. S134E phosphomimetic hSSB1 binds DNA similarly to WT

In the above sections we have demonstrated that hSSB1 S134 is dynamically phosphorylated and that this modification promotes cellular survival in response to replication fork disruption, as well as double-strand DNA break formation. It was therefore interesting to consider how S134 phosphorylation may affect the molecular function of hSSB1.

The C-terminal tail of hSSB1 was recently described as important for efficient DNA-binding [29]. The position of S134 at the start of this region therefore raised the possibility that phosphorylation of this residue may alter the interaction of hSSB1 with DNA. To assess this, recombinant WT and S134E hexa-His-hSSB1 was purified from *E. coli* and the ssDNA-binding capacity of each protein measured using BioLayer interferometry (BLI). Although hSSB1 has previously being described as an ssDNA-binding protein with negligible affinity for dsDNA [14,30], we also assessed the binding of WT and S134E hSSB1 to a fork junction substrate lacking exposed ssDNA [20], representing a structure likely to form in the processing of disrupted replication forks. Whilst hSSB1 was indeed able to bind a fork junction substrate, albeit with lower affinity than ssDNA, we however did not detect any statistically significant difference in binding between WT and S134E hSSB1 for either substrate (Fig. 6). These data thereby suggest an alteration of DNA-binding activity is an unlikely function of hSSB1 S134 phosphorylation.

4. Discussion

Enzymatically active DNA-PK is a central component of the cellular response to replication fork inhibition [6]. For instance, cells depleted of endogenous DNA-PKcs or expressing an enzymatically deficient kinase mutant are unable to efficiently restart stalled replication forks and show reduced clonogenic survival when treated with hydroxyurea [7]. With the notable exception of RPA32 [8], as well as of autophosphorylation [7], few relevant DNA-PK substrates have however been identified in response to replication stress. In this article we demonstrate that hSSB1 S134 phosphorylation is required for clonogenic survival of cells treated with the replication stress compounds hydroxyurea, aphidicolin and camptothecin, as well as establish that phosphorylation is primarily a result of DNA-PK activity. As a small decrease in hSSB1 S134 phosphorylation was also observed following the inhibition of ATM and ATR, we cannot however exclude that these kinases may also contribute a small amount to the phosphorylation of

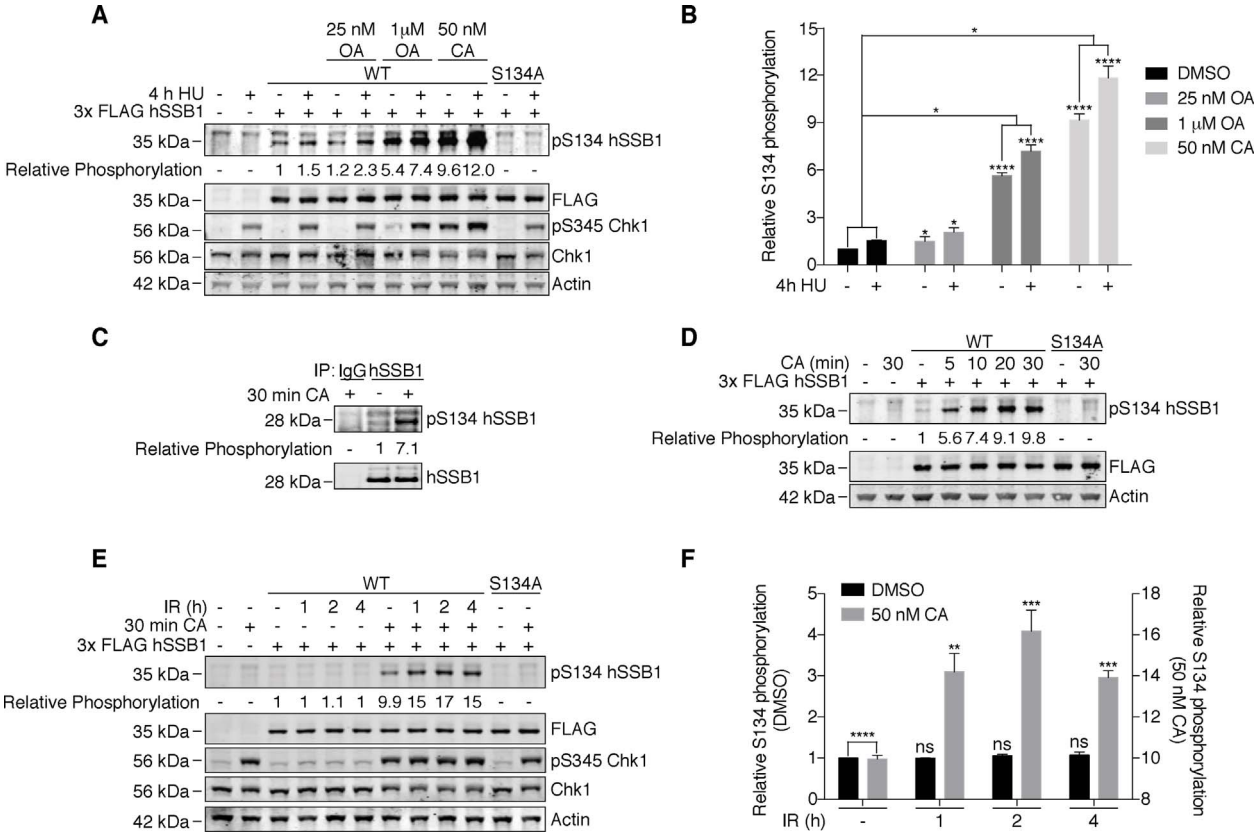

Fig. 5. hSSB1 S134 phosphorylation is regulated by PPP-family protein phosphatases. **(A)** HeLa cells transiently expressing WT or S134A 3x FLAG hSSB1, or an empty vector, for 24 h were treated with 3 mM HU for 3.5 h prior to addition of 25 nM okadaic acid (OA), 1 μM OA, or 50 nM calyculin A (CA) for 30 min. Whole cell lysates were prepared and immunoblotted for phosphorylation of hSSB1 S134. Phosphorylation of hSSB1 S134 is expressed relative to 3x FLAG hSSB1. **(B)** Bar graph illustrating the relative levels of hSSB1 S134 phosphorylation from three independent repeats of **(A)**. Data is graphed as the mean ± 1 standard deviation. *t* tests were used to compare phosphorylation of hSSB1 S134 for each inhibitor data set relative to DMSO lanes for untreated and 3 mM HU treated samples (above the bars). *t* tests were also used to compare the HU-induced increase in S134 phosphorylation following phosphatase treatment (above the lines) * = $p < 0.05$, ** = $p < 0.01$, *** = $p < 0.001$, **** = $p < 0.0001$. **(C)** hSSB1 was immunoprecipitated from HeLa cells that had been treated with 50 nM CA for 30 min, or mock-treated. Eluted proteins were immunoblotted for total and S134 phosphorylated hSSB1. Phosphorylation of hSSB1 S134 is expressed relative to total immunoprecipitated endogenous hSSB1. **(D)** HeLa cells expressing WT or S134A 3x FLAG hSSB1 were treated with 50 nM CA for 5, 10, 20 or 30 min. Whole cell lysates were prepared and analysed by immunoblotting. Phosphorylation of hSSB1 S134 is expressed relative to 3x FLAG hSSB1. **(E)** HeLa cells transiently expressing WT or S134A 3x FLAG hSSB1, or an empty vector, for 24 h were either left untreated or exposed to 6 Gy of ionising radiation and harvested after 1, 2 or 4 h. Thirty minutes prior to harvesting, cells were also treated ± 50 nM CA. Whole cell lysates were prepared and immunoblotted for phosphorylation of hSSB1 S134, which is expressed relative to 3x FLAG hSSB1. **(F)** Bar graph illustrating the relative levels of hSSB1 S134 phosphorylation from three independent repeats of (G). Data is graphed as the mean ± 1 standard deviation. *t* tests were used to compare phosphorylation of hSSB1 S134 from those cells exposed to ionising radiation with the unexposed lanes within each data set (± CA) A *t test* was also used to compare phosphorylation of hSSB1 S134 from CA treated and untreated non-irradiated cells. ns = non significant, * = $p < 0.05$, ** = $p < 0.01$, *** = $p < 0.001$, **** = $p < 0.0001$.

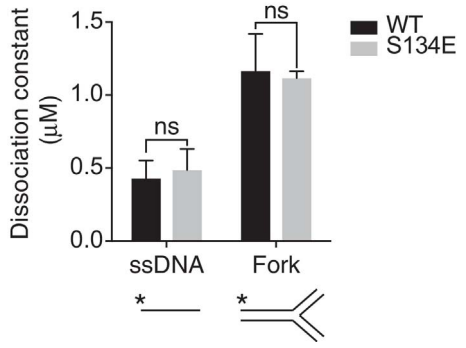

Fig. 6. S134E phosphomimetic hSSB1 binds DNA similarly to WT DNA binding of WT and S134E recombinant hexa-His-hSSB1 was assessed by BioLayer interferometry and the dissociation constants of each protein for single-stranded and fork DNA substrates determined. Data is graphed as the mean ± 1 standard deviation. *t* tests were used to compare the dissociation constants for each substrate. ns = non significant ($p > 0.05$). The schematics below each pair of columns represent the tested DNA substrates where * = biotin.

hSSB1 S134. Such overlap is consistent with previous studies on other known PI3K-like kinase substrates and is exemplified by the overlapping ATM and DNA-PK phosphorylation of RPA32 residues S4/8 and S12 [8], as well as the ATM and DNA-PK phosphorylation of Chk1 S317 in cells where ATR (the predominant kinase of Chk1 S317) function is suppressed (25). Alternatively, the reduction in hSSB1 S134 phosphorylation observed following ATM and ATR inhibition might result from indirect de-regulation of DNA-PK function. Indeed, the phosphorylation and thereby activation of DNA-PK by ATM [31] and ATR [32] has previously been demonstrated, the disruption of which might also explain the small reduction in hSSB1 S134 phosphorylation observed following inhibition of these enzymes.

While hSSB1 S134 is also phosphorylated by DNA-PK in undamaged cells, this may be maintained at steady-state levels by the opposing activities of PPP-family protein phosphatases. This family includes numerous members that are inhibited by okadaic acid in cells, including PP2A, PP4, PP5, and PP6 (23). The increase in hSSB1 phosphorylation observed following treatment with okadaic acid therefore suggests the involvement of one of these enzymes in the de-phosphorylation of hSSB1. Indeed, each of these enzymes has previously been implicated in the regulation of DNA repair pathways [33] and may represent plausible regulators of hSSB1. Although we did observe an additional

increase in hSSB1 phosphorylation when calcyculin A was added to cells, a compound that also inhibits PP1, it is unclear whether the greater affect observed here with comparison to okadaic acid treatment is due to PP1 involvement. Indeed, calyculin A also shows increased potency towards PP5, the involvement of which also represents a plausible explanation. Further studies will therefore be required to establish which PPP-family members are involved in dephosphorylating hSSB1 S134. Such experiments, which would likely require the specific depletion of individual PPP-family member subunits, may however be hampered by potential indirect affects which may arise due to disruption of dephosphorylation events required for proper regulation of DNA-PK or of DNA-PK regulatory proteins. Indeed, we cannot exclude the possibility that such indirect affects may account for some of the increased hSSB1 S134 phosphorylation observed here following calyculin A and okadaic acid treatment. In addition, as both of these compounds are know to have cytotoxic affects on cells [34], we cannot exclude, based on our data, that hSSB1 S134 may be phosphorylated as a result of these cellular changes, independently of direct disruption of dynamic phosphorylation.

It is of interest to consider an explanation for the apparent phosphorylation of hSSB1 in undamaged cells. One such may be that in order to execute a rapid response to replication inhibition, basal S134 phosphorylation could function to keep hSSB1 in a 'primed' state prior to stress. Such an arrangement may be consistent with our previous description of hSSB1 as an early responder to DNA damage. This is demonstrated by the rapid co-localisation of hSSB1 with sites of stalled replication in response to hydroxyurea treatment and its subsequent roles in ATR recruitment [11]. A similar 'priming' approach has also been suggested for Chk1, where phosphorylation of S317 and S345 is maintained under a suppressive state by PP1 during un-perturbed cell cycles to allow for rapid checkpoint activation in response to replication fork stalling [27]. As basal hSSB1 phosphorylation may involve DNA-PK function, this scenario suggests that a pool of activated DNA-PK must also exist in un-exogenously damaged cells. This is supported by the similar increase in DNA-PK auto-phosphorylation that has been observed following okadaic acid treatment of cells [35], or depletion of PP5 [33]. It is worth noting, however, that basal phosphorylation of RPA32 S33 was also observed in cells, which increased at a similar rate to hSSB1 S134 phosphorylation following hydroxyurea treatment. RPA32 S33 phosphorylation in undamaged cells has previously been found to occur in the late S- and G2 phases of the cell cycle and has been attributed to the persistence of endogenously stalled replication forks [24]. A similar regulatory mechanism may thereby also explain the detection of S134 phosphorylated hSSB1 in undamaged cells. As detection of S134 phosphorylation predominantly required transient overexpression of hSSB1, we cannot however rule out that the high degree of basal hSSB1 phosphorylation observed was due the equilibrium between S134 phosphorylation and de-phosphorylation being somewhat altered from endogenous ratios.

Whilst our studies of WT and S134E hSSB1 DNA-binding did not yield any additional insight into the molecular function of S134 phosphorylation, we were surprised to find that hSSB1 can bind fork substrates, especially given the negligible interaction of hSSB1 with dsDNA duplexes reported previously [14]. Interestingly, a similar observation was recently reported for the annealing helicase SMARCAL1, a protein that also has minimal affinity for dsDNA, although which readily binds model replication forks lacking exposed ssDNA [36]. In this work, the authors suggested SMARCAL1 might capture small amounts of ssDNA that are exposed due to 'breathing' of the dsDNA regions adjacent to the fork junction. It is tempting to consider that hSSB1 may bind this structure through a similar means. Indeed, these results are somewhat reminiscent of our finding that hSSB1 is able to bind a dsDNA substrate containing a single 8-oxoguanine modification, potentially due to a similar localised de-stabilisation of the DNA duplex [14]. Although we have previously demonstrated that hSSB1 localises to replication forks following their disruption [11], the mechanistic consequence of fork-junction binding however remains unclear. These data nevertheless suggest that S134 phosphorylation is unlikely to alter hSSB1 DNA-binding and may instead alter hSSB1 via an alternative means, such as by modulating the interaction with an as yet unidentified protein-binding partner.

We were also interested to note that despite the lack of site-specific conservation of an SQ motif at S134 outside of primates, numerous other animal species also contain SQ/TQ motifs within an ~ 40 amino acid region homologous to hSSB1 residues 117–160. This includes in distantly related animals, such as in reptiles, amphibians and fish. Although the modification of these putative PI3K-like kinase phosphorylation motifs remains unexplored, the presence of these motifs in the vast majority of species examined may suggest that despite low specific conservation of hSSB1 S134 (or T117), selective pressure may exist for the occurrence of phosphorylation sites within this region of SSB1 homologues. Whether these additional SQ/TQ motifs are indeed phosphorylated and alter SSB1 function by a means similar to S134 phosphorylation, will however require additional experimentation.

In summary, the data presented here indicate that hSSB1 phosphorylation at S134 is dynamically regulated by DNA-PK and PPP-family protein phosphatases. Furthermore, this modification is enhanced following replication inhibition and promotes hSSB1-mediated cell survival. These data thereby suggest a novel mechanism utilised by cells in the response to DNA damage. As such stress is induced by numerous chemotherapeutics, the disruption of hSSB1 S134 phosphorylation may therefore represent an effective target for the sensitisation of cancer cells.

Conflict of interest

The authors declare that they have no conflicts of interest

Author contributions

NWA, NP, EB, PP and DJR designed the experiments, the majority of which were performed by NWA. SLS performed LC-MS/MS and analysed the resulting data together with CB. CT, RK, AF and RG purified recombinant protein and performed 1D NMR and the BLI studies with assistance from LC. NWA wrote the paper with suggestions from NP, SLS, EB, RG, LC, PP, DJR and KJO. All authors read and approved the final version of the manuscript.

Acknowledgments

This work was supported by a National Health and Medical Research Council project grant [1066550], an Australian Research Council project grant [DP 120103099] and by a Queensland Health Senior Clinical Research Fellowship awarded to K.J.O. This work was also supported by the Wellcome Trust [094476/Z/10/Z], which funded the purchase of the TripleTOF 5600 mass spectrometer at the BSRC Mass Spectrometry and Proteomics Facility, University of St Andrews. NWA was supported by a scholarship awarded by Cancer Council Queensland. E.B. is supported by an Advance Queensland Research Fellowship. The author's wish to acknowledge Samuel Beard, Joshua Burgess and Mark Adams for assistance in the generation of preliminary data associated with this manuscript.

Appendix A. Supplementary data

Supplementary data associated with this article can be found, in the online version, at http://dx.doi.org/10.1016/j.dnarep.2017.03.006.

References

[1] D. Branzei, M. Foiani, The DNA damage response during DNA replication, Curr. Opin. Cell Biol. 17 (2005) 568–575, http://dx.doi.org/10.1016/j.ceb.2005.09.003.

[2] L.I. Toledo, M. Altmeyer, M.-B. Rask, C. Lukas, D.H. Larsen, L.K. Povlsen, et al., ATR prohibits replication catastrophe by preventing global exhaustion of RPA, Cell 155 (2013) 1088–1103, http://dx.doi.org/10.1016/j.cell.2013.10.043.
[3] H.L. Ball, J.S. Myers, D. Cortez, ATRIP binding to replication protein a-single-stranded DNA promotes ATR-ATRIP localization but is dispensable for Chk1 phosphorylation, Mol. Biol. Cell. 16 (2005) 2372–2381, http://dx.doi.org/10.1091/mbc.E04-11-1006.
[4] H. Zhao, H. Piwnica-Worms, ATR-mediated checkpoint pathways regulate phosphorylation and activation of human Chk1, Mol. Cell. Biol. 21 (2001) 4129–4139, http://dx.doi.org/10.1128/MCB.21.13.4129-4139.2001.
[5] F.B. Couch, C.E. Bansbach, R. Driscoll, J.W. Luzwick, G.G. Glick, R. Bétous, et al., ATR phosphorylates SMARCAL1 to prevent replication fork collapse, Genes Dev. 27 (2013) 1610–1623, http://dx.doi.org/10.1101/gad.214080.113.
[6] Y.-F. Lin, H.-Y. Shih, Z. Shang, S. Matsunaga, B.P. Chen, DNA-PKcs is required to maintain stability of Chk1 and Claspin for optimal replication stress response, Nucleic Acids Res. 42 (2014) 4463–4473, http://dx.doi.org/10.1093/nar/gku116.
[7] S. Ying, Z. Chen, A.L. Medhurst, J.A. Neal, Z. Bao, O. Mortusewicz, et al., DNA-PKcs and PARP1 bind to unresected stalled DNA replication forks where they recruit XRCC1 to mediate repair, Cancer Res. 76 (2016) 1078–1088, http://dx.doi.org/10.1158/0008-5472.CAN-15-0608.
[8] S. Liu, S.O. Opiyo, K. Manthey, J.G. Glanzer, A.K. Ashley, C. Amerin, et al., Distinct roles for DNA-PK, ATM and ATR in RPA phosphorylation and checkpoint activation in response to replication stress, Nucleic Acids Res. 40 (2012) 10780–10794, http://dx.doi.org/10.1093/nar/gks849.
[9] R.G. Shao, C.X. Cao, H. Zhang, K.W. Kohn, M.S. Wold, Y. Pommier, Replication-mediated DNA damage by camptothecin induces phosphorylation of RPA by DNA-dependent protein kinase and dissociates RPA:DNA-PK complexes, Embo J. 18 (1999) 1397–1406, http://dx.doi.org/10.1093/emboj/18.5 1397.
[10] R.W. Anantha, V.M. Vassin, J.A. Borowiec, Sequential and synergistic modification of human RPA stimulates chromosomal DNA repair, J. Biol. Chem. 282 (2007) 35910–35923, http://dx.doi.org/10.1074/jbc.M704645200.
[11] E. Bolderson, E. Petermann, L. Croft, A. Suraweera, R.K. Pandita, T.K. Pandita, et al., Human single-stranded DNA binding protein 1 (hSSB1/NABP2) is required for the stability and repair of stalled replication forks, Nucleic Acids Res. 42 (2014) 6326–6336, http://dx.doi.org/10.1093/nar/gku276.
[12] A. Kar, M. Kaur, T. Ghosh, M.M. Khan, A. Sharma, R. Shekhar, et al., RPA70 depletion induces hSSB1/2-INTS3 complex to initiate ATR signaling, Nucleic Acids Res. 43 (2015) 4962–4974, http://dx.doi.org/10.1093/nar/gkv369.
[13] D.J. Richard, E. Bolderson, L. Cubeddu, R.I.M. Wadsworth, K. Savage, G.G. Sharma, et al., Single-stranded DNA-binding protein hSSB1 is critical for genomic stability, Nature 453 (2008) 677–681, http://dx.doi.org/10.1038/nature06883.
[14] N. Paquet, M.N. Adams, V. Leong, N.W. Ashton, C. Touma, R. Gamsjaeger, et al., hSSB1 (NABP2/OBFC2B) is required for the repair of 8-oxo-guanine by the hOGG1-mediated base excision repair pathway, Nucleic Acids Res. 43 (2015) 8817–8829, http://dx.doi.org/10.1093/nar/gkv790.
[15] Y. Wu, H. Chen, J. Lu, M. Zhang, R. Zhang, T. Duan, et al., Acetylation-dependent function of human single-stranded DNA binding protein 1, Nucleic Acids Res. 43 (2015) 7878–7887, http://dx.doi.org/10.1093/nar/gkv707.
[16] P.V. Hornbeck, B. Zhang, B. Murray, J.M. Kornhauser, V. Latham, E. Skrzypek, PhosphoSitePlus 2014 mutations, PTMs and recalibrations, Nucleic Acids Res. 43 (2015) D512–D520, http://dx.doi.org/10.1093/nar/gku1267.
[17] N. Paquet, J.K. Box, N.W. Ashton, A. Suraweera, L.V. Croft, A.J. Urquhart, et al., Néstor-Guillermo progeria syndrome: a biochemical insight into barrier-to-auto-integration factor 1, alanine 12 threonine mutation, BMC Mol. Biol. 15 (2014) 27, http://dx.doi.org/10.1186/s12867-014-0027-z.
[18] A. Shevchenko, M. Wilm, O. Vorm, M. Mann, Mass spectrometric sequencing of proteins silver-stained polyacrylamide gels, Anal. Chem. 68 (1996) 850–858.
[19] J.A. Vizcaíno, A. Csordas, N. del-Toro, J.A. Dianes, J. Griss, I. Lavidas, et al., 2016 update of the PRIDE database and its related tools, Nucleic Acids Res. 44 (2016) D447–D456, http://dx.doi.org/10.1093/nar/gkv1145.
[20] V. Marini, L. Krejci, Unwinding of synthetic replication and recombination substrates by Srs2, DNA Repair (Amst.). 11 (2012) 789–798, http://dx.doi.org/10.1016/j.dnarep.2012.05.007.
[21] R. Prakash, D. Satory, E. Dray, A. Papusha, J. Scheller, W. Kramer, et al., Yeast Mph1 helicase dissociates Rad51-made D-loops: implications for crossover control in mitotic recombination, Genes Dev. 23 (2009) 67–79, http://dx.doi.org/10.1101/gad.1737809.
[22] A. Koç, L.J. Wheeler, C.K. Mathews, G.F. Merrill, Hydroxyurea arrests DNA replication by a mechanism that preserves basal dNTP pools, J. Biol. Chem. 279 (2004) 223–230, http://dx.doi.org/10.1074/jbc.M303952200.
[23] N. Feldhahn, E. Ferretti, D.F. Robbiani, E. Callen, S. Deroubaix, L. Selleri, et al., The hSSB1 orthologue Obfc2b is essential for skeletogenesis but dispensable for the DNA damage response in vivo, Embo J. 31 (2012) 4045–4056, http://dx.doi.org/10.1038/emboj.2012.247.
[24] V.M. Vassin, R.W. Anantha, E. Sokolova, S. Kanner, J.A. Borowiec, Human RPA phosphorylation by ATR stimulates DNA synthesis and prevents ssDNA accumulation during DNA-replication stress, J. Cell. Sci. 122 (2009) 4070–4080, http://dx.doi.org/10.1242/jcs.053702.
[25] C.J. Bakkenist, M.B. Kastan, DNA damage activates ATM through intermolecular autophosphorylation and dimer dissociation, Nature 421 (2003) 499–506, http://dx.doi.org/10.1038/nature01368.
[26] A.A. Goodarzi, J.C. Jonnalagadda, P. Douglas, D. Young, R. Ye, G.B.G. Moorhead, et al., Autophosphorylation of ataxia-telangiectasia mutated is regulated by protein phosphatase 2A, Embo J. 23 (2004) 4451–4461, http://dx.doi.org/10.1038/sj.emboj.7600455.
[27] V. Leung-Pineda, C.E. Ryan, H. Piwnica-Worms, Phosphorylation of Chk1 by ATR is antagonized by a Chk1-regulated protein phosphatase 2A circuit, Mol. Cell. Biol. 26 (2006) 7529–7538, http://dx.doi.org/10.1128/MCB00447-06.
[28] B. Favre, P. Turowski, B.A. Hemmings, Differential inhibition and posttranslational modification of protein phosphatase 1 and 2A in MCF7 cells treated with calyculin-A, okadaic acid, and tautomycin, J. Biol. Chem. 272 (1997) 13856–13863.
[29] V. Vidhyasagar, Y. He, M. Guo, H. Ding, T. Talwar, V. Nguyen, et al., C-termini are essential and distinct for nucleic acid binding of human NABP1 and NABP2, Biochim. Biophys. Acta. 1860 (2016) 371–383, http://dx.doi.org/10.1016/j.bbagen.2015.11.003.
[30] D.J. Richard, K. Savage, E. Bolderson, L. Cubeddu, S. So, M. Ghita, et al., hSSB1 rapidly binds at the sites of DNA double-strand breaks and is required for the efficient recruitment of the MRN complex, Nucleic Acids Res. 39 (2011) 1692–1702, http://dx.doi.org/10.1093/nar/gkq1098.
[31] B.P.C. Chen, N. Uematsu, J. Kobayashi, Y. Lerenthal, A. Krempler, H. Yajima, et al., Ataxia telangiectasia mutated (ATM) is essential for DNA-PKcs phosphorylations at the Thr-2609 cluster upon DNA double strand break, J. Biol. Chem. 282 (2007) 6582–6587, http://dx.doi.org/10.1074/jbc.M611605200.
[32] H. Yajima, K.-J. Lee, B.P.C. Chen, ATR-dependent phosphorylation of DNA-dependent protein kinase catalytic subunit in response to UV-induced replication stress, Mol. Cell. Biol. 26 (2006) 7520–7528, http://dx.doi.org/10.1128/MCB00048-06.
[33] T. Wechsler, B.P.C. Chen, R. Harper, K. Morotomi-Yano, B.C.B. Huang, K. Meek, et al., DNA-PKcs function regulated specifically by protein phosphatase 5, Proc. Natl. Acad. Sci. USA 101 (2004) 1247–1252DOI 10.1073/pnas.0307765100.
[34] Y. Morimoto, T. Ohba, S. Kobayashi, T. Haneji, The protein phosphatase inhibitors okadaic acid and calyculin A induce apoptosis in human osteoblastic cells, Exp. Cell Res. 230 (1997) 181–186, http://dx.doi.org/10.1006/excr.1996.3404.
[35] P. Douglas, G.P. Sapkota, N. Morrice, Y. Yu, A.A. Goodarzi, D. Merkle, et al., Identification of in vitro and in vivo phosphorylation sites in the catalytic subunit of the DNA-dependent protein kinase, Biochem. J. 368 (2002) 243–251, http://dx.doi.org/10.1042/BJ20020973.
[36] R. Bétous, A.C. Mason, R.P. Rambo, C.E. Bansbach, A. Badu-Nkansah, B.M. Sirbu, et al., SMARCAL1 catalyzes fork regression and Holliday junction migration to maintain genome stability during DNA replication, Genes Dev. 26 (2012) 151–162, http://dx.doi.org/10.1101/gad.178459.111.